Integrated Multifunctional Electrochemistry Microchip for Highly Efficient Capture, Release, Lysis, and Analysis of Circulating Tumor Cells

Shuangqian Yan,[†,§] Peng Chen,[†,§] Xuemei Zeng,[†] Xian Zhang,[†] Yiwei Li,[†] Yun Xia,[†] Jie Wang,[†] Xiaofang Dai,[‡] Xiaojun Feng,[†] Wei Du,[†] and Bi-Feng Liu*,[†]

[†]The Key Laboratory for Biomedical Photonics of MOE at Wuhan National Laboratory for Optoelectronics—Hubei Bioinformatics & Molecular Imaging Key Laboratory, Systems Biology Theme, Department of Biomedical Engineering, College of Life Science and Technology, Huazhong University of Science and Technology, Wuhan 430074, China

[‡]Cancer Center, Tongji Medical College, Huazhong University of Science and Technology, Wuhan 430074, China

S *Supporting Information*

ABSTRACT: The circulating tumor cells (CTCs) in the blood allow the noninvasive analysis of metastatic mechanisms, cancer diagnosis, prognosis, disease monitoring, and precise therapy through "liquid biopsies". However, there is no integrated and robust multifunctional microchip, which not only could highly efficient capture CTCs, but also fast release and lyse cells on one single chip without using other biochemical agents for downstream biomedical analysis. In this work, we integrated the three functions in one electrochemical microchip (echip) by intentionally designing a cactus-like, topologically structured conductive array consisted of a PDMS micropillar-array core and an electro-conductive gold coating layer with hierarchical structure. The echip presented a capture efficiency of 85−100% for different cell lines in both buffer solution and whole blood. Moreover, the validity of the echip was further evaluated by using non-small-cell lung cancer patient samples. The electrochemical released cells or lysed-cell solutions could be obtained within 10 min and have been successfully used for mutant detection by DNA sequencing or RT-PCR. The fast release at a relative low voltage (−1.2 V) was originating from an electrochemical cleavage of the Au−S bonds that immobilized antibody on the chip. The electrochemical lysis took place at a high voltage (20 V) with an admirable performance. Thus, the highly integrated multifunctional echip was well demonstrated and promised a significant application in the clinical field.
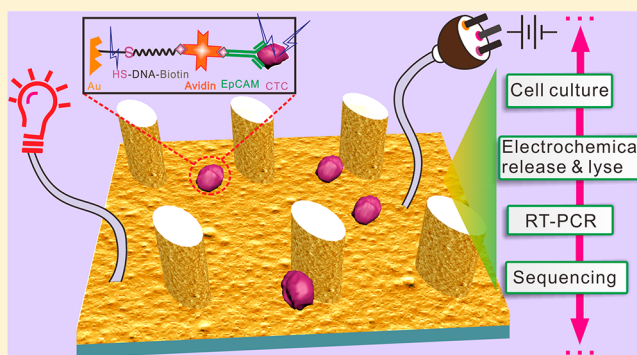
The metastasis of tumor cells to distant locations from the primary causes 90% cancer related deaths.[1] The circulating tumor cells (CTCs) in the blood may allow the noninvasive analysis of the metastatic mechanisms, cancer diagnosis, prognosis, disease monitoring, and precise therapy through "liquid biopsies".[2−6] However, CTCs are extremely rare in the bloodstream, only several to hundreds of cells per mL, therefore presenting the first challenge of CTCs analysis, which is how to isolate the disseminated tumor cells with high efficiency.[7] Moreover, the downstream biological analysis needs adequate analyte and also good cell viability, so the highly efficient release with intact cells is a more significant challenge, especially for clinical applications in which the robustness, the conveniency of the fabrication process and the cost of the device are also the extremely important concerns.[8] However, there are few progresses in the CTCs study meet all these challenges simultaneously. Tremendous progresses have been made for improving the capture efficiency,[9−19] especially by combining the nanomaterials with microfluidics.[20−24] Never-

theless, for the downstream biomedical analysis, the highly efficient release with intact cells is undoubtedly expected.[25] However, traditionally the cell release often relies on the enzymes or other chemicals which may severely influence the cell viability.[26−29] Additionally, the cell collection and off-chip cell lysis may cause the loss of rare cells, dramatically affecting the downstream analysis. Considering the current situations in the field, a highly integrated and robust microchip that could capture, release and lyse CTCs on-chip with high efficiency via a disruptive and convenient method is quite desired.[30,31]

In this article, we fabricated an electrochemical microchip (echip) for highly efficient capture, electrochemical release, and on-chip lysis of the CTCs. The echip is made up of a hierarchical structured micropillar arrays and a glass slide. The PDMS micropillar array was fabricated from PDMS substrate
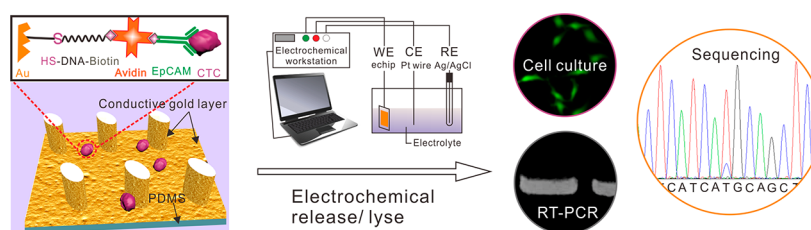
Figure 1. Schematic illustration of the echip. Thiol-gold binding and avidin−biotin strategy for modifying EpCAM-specific monoclonal antibodies; Conductive gold layer mainly responsible for the electrochemical release and lysis of the captured cells.

by the conventional soft-lithography technology and then plated a gold layer by electroless plating method.[17] The electroconductive gold layer possessed hierarchical structures from micrometer to nanometer scale and could be applied to electrochemically release and lyse the captured cells for downstream biological studies (Figure 1). Compared with CELLSEARCH system, our echip has higher CTCs capture performance. More importantly, it provides an integrated approach or solution for CTCs capture, counting, release, and lysis, which is definitely more suitable for clinic.

■ EXPERIMENTAL SECTION

Reagents and Instruments. Calcein-AM, avidin, KHCO₃, 4,6-diamidino-2-phenylindole (DAPI), bovine serum albumin (BSA), and TCEP (tris(2-carboxyethyl)phosphine) were purchased from Sigma-Aldrich, Inc. (U.S.A.). HAuCl₄·3H₂O and glucose were obtained from Sinopharm Chemical Reagent (Shanghai, China). Anti-CD45 (FITC) and anticytokeratin (PE) were bought from BD Biosciences (U.S.A). Anti-EpCAM (biotin) was purchased from Abcam. Oligonucleotide was obtained from Sangon Biotech (Shanghai). Human breast cancer cells (MCF-7) was a gift from the Dr. Shuai Xia. Human cervical carcinoma cells (HeLa), prostatic cancer cells (PC3), hepatocellular carcinoma cells (HepG2), and human non-small-cell lung cancer cells (NCI-H1650) were purchased from Wuhan finetest biotech (China). Sylgard 184 including polydimethylsiloxane (PDMS) monomer and curing agent was purchased from Dow Corning (Midland, MI, U.S.A.). All the media for cell culture were bought from Gibco Corp. Human blood samples were supplied by Wuhan Union Hospital. Ultrapure water (18 MΩ·cm) was made by a Millipore Milli-Q system. Scanning electron microscope (Nano SEM, Tecnai G20, Netherlands); atom force microscope (AFM, SPM9700, SHIMADZU, Japan); fluorescence microscope (Zeiss Axio Zoom. V16 or Olympus America, Melville, NY, USA); X Ray diffracmeter (Empyrean, PAN-alytical B.V. Netherlands); Electrochemical workstation (CHI660E, Shanghai, China).

Cell Culture. PC3 cell was cultured in Ham's F-12K (Kaighn's) Medium. MCF-7 and NCI-H1650 cells were cultured in RPMI medium 1640 (Fisher Scientific). HeLa and HepG2 cells were cultured in DMEM medium. All cell culture media were supplemented with 10% fetal bovine serum (FBS; heat-inactivated; Gibco) and 100 units/mL penicillin streptomycin (Gibco). All cultures were incubated at 37 °C under a 5% CO₂ atmosphere. Dulbecco's phosphate-buffered saline with calcium and magnesium (Fisher Scientific, USA) was used to wash cells.

Devices Fabrication and Modification. The devices fabrication and modification were conducted according to our previous literature with slightly modify.[17] Briefly, the PDMS

micropillar array (dimension of the channel was 40 mm in length and 20 mm in width) was fabricated by conventional soft lithography method. And then, we conformally plated gold layer on the array. In details, the edges of the PDMS microarray were protected with thin PDMS slices to prevent gold deposition. And then, the edges protected PDMS array was aminated with the APTES solution (volume ratio, ethyl alcohol/water/APTES = 50:5:2.5) about 30 min after treated with oxygen plasma for 1 min. After it was rinsed with ethyl alcohol and water several times, the PDMS array was placed onto a PDMS frame that contained the plating solution (containing 0.5% (w/v) HAuCl₄, 0.05 g mL⁻¹ KHCO₃, and 5 mg mL⁻¹ glucose), allowing the array in contact with the plating solution for gold deposition in dark room at ambient temperature for about 6 h. The gold deposited microarray was rinsed with ethyl alcohol and water several times and dried by nitrogen. Inlet and outlet were punched at middle of two ends of the PDMS microarray. And at the two corner of PDMS microarray, two holes were punched to insert silver wires to make the echip could be conduct the electrode of the electrochemical workstation. At last, PDMS microarray was bonded onto a glass slide by plasma treatment to form the final echip.

For the antibodies modification, oligonucleotide (5′-HS-TTTTTTTTTT-biotin-3′) assembled on the gold layer surface through the gold−thiol chemistry. Following avidin and biotinylated EpCAM-specific monoclonal antibodies were modified. Whole echip channel was blocked with 1% BSA and stored at 4 °C with high humidity.

Cell Capture. The process of cell capture was conducted according to our previous literature.[17] Briefly, a given number of fluorescently labeled cells was pipetted to the 1 mL of PBS or whole blood in 1 mL syringe and mixed at least 3 min by a tiny magnetic stirring bar placed inside the syringe before introduction into the echip by a Micro4 syringe pump that could well control the flow rate. The magnetic stirring bar was kept working to prevent the cell precipitation while the cell mixture was being pumped through the chip. For the blood samples, the captured cells were washed with PBS, fixed with 4% paraformaldehyde (PFA), permeabilized with 0.2% Triton-X and incubated for 30 min followed by a PBS wash and blocking the chip with 3% BSA. Anticytokeratin (PE), anti-CD45 (FITC), and DAPI were used to stain the cancer cells, leukocytes and nuclei, respectively. To determine cell number, the echip was placed on the stage of a fluorescence microscope to capture images at different fluorescence channel. The microchip was scanned automatically under an inverted microscope (objective lens, 60×). The cell debris and nonspecific cells were excluded according to size, shape and the nuclear size. The images were analyzed by Image-Pro Plus to count the cell number. Cells with positive staining for
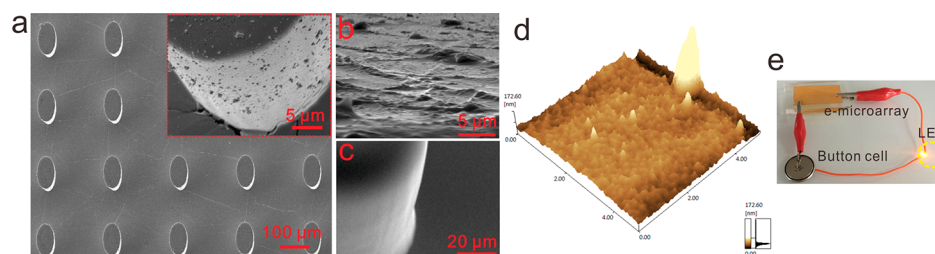
Figure 2. Characterization of echip. (a) SEM image of gold layer coated micropillar array. Inset: Close-up view of single gold layer coated micropillar. (b) SEM image of micro/nanostructures on channel bottom. (c) SEM image of micropillar without gold layer coating. (d) AFM image of topological structures on channel after gold deposition. (e) Photo of the gold layer coated microarray connected with a LED and a button cell.
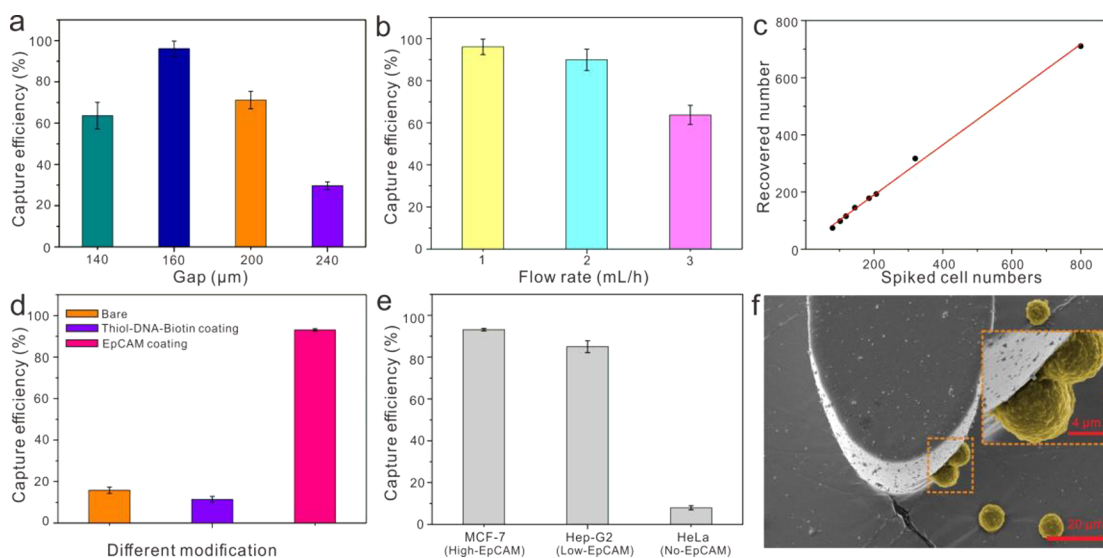
Figure 3. Optimization and characterization of the echip in buffer system. (a) Cell-capture efficiency of the EpCAM-coated echip at micropillar gap of 140, 160, 200, and 240 μm. (b) Cell-capture efficiency of the EpCAM-coated echip at flow rates of 1, 2, and 3 mL h^{-1}. (c) Capture efficiency of MCF-7 cells at 2 mL h^{-1}. A linear fitting of the data (red solid line). (d) Comparison of the capture efficiency for MCF-7 cells using bare, thiol-DNA-biotin-coated, and anti-EpCAM-modified echip. (e) Comparison of different cell lines: MCF-7 cells (high EpCAM expression), HepG2 cells (low EpCAM expression), and HeLa cells (no EpCAM expression). (f) SEM image of the captured MCF-7 cells.

cytokeratin (cytokeratin$^+$, DAPI$^+$, and CD45$^-$) and matching the phenotypic morphological characteristics were scored as cancer cells.

Cell Release and Lyse with Electrochemical Method. For better connect the echip, two gold slices were inserted into the two side of the echip channel. To release the captured cells, we used the echip as work electrode, Pt wire counter electrode, Ag/AgCl conference electrode and immersed those electrodes into PBS buffer (pH 7.4). After reduction of the thiol−Au bond at voltage of −1.2 V for 10 min, the solution in echip channel was collected. To lyse the captured cells, 20 V voltage was applied for 10 min. The electrochemical lysis based on electrochemically generate hydroxyl ions which permeabilize and break the cell lipid bilayer. The procedures of RT-PCR and sequencing assay were according to the previous literatures.[10,22]

■ RESULTS AND DISCUSSION

Figure 2a and 2b showed the SEM images of the gold layer-coated elliptic microarray. The XRD pattern of the gold layer was shown in Figure S1 and revealed numerous hierarchical structures on the micropillar (100 μm × 50 μm (a × b)) and the echip channel (Figure S2−S4), while the PDMS micropillar without gold coating layer presented a smooth surface (Figure 2c). Nanostructures was also observed on the bottom of micropillars as shown in the AFM images of Figure 2d and

Figure S5, which could offer high specific surface area for antibody immobilization and extra physical cues to interact with the cancer cells. Differing from our previous work,[17] the PDMS micropillar was aminated with the APTES before plating the gold layer. The amination enables the deposition of a thicker gold layer, leading to a hierarchically structured and electro-conductive micropillar array (Figure 2e). More interesting is that the gold coated microarray could be bended and twisted without affecting its electroconductivity (Figure S6), thus confirming the significant robustness of our echip.

There are about 25 000 elliptic pillars with equilateral triangular arrangement in the channel of echip and the simulation result of flow profile for the microarray was illustrated in Figure S7. To increase the capture efficiency, the breast cancer cell (MCF-7) was used to optimize the micropillar gap (distance) and flow rate. As illustrated in Figure 3a, the capture efficiency at flow rate of 1 mL/h was increased from 63.6% to 96.1% when gap was increased from 140 to 160 μm, while it decreased significantly when gap reaches up to 200 μm (71.2%). More significant decrease can be seen at the gap of 240 μm (29.6%). And then the flow rate was optimized at gap of 160 μm. At the flow rate of 1, 2, and 3 mL/h, the capture efficiency was 96.1%, 89.9%, and 63.7%, respectively, which is presumably owing to the increased shear stress as the flow rate increasing (Figure 3b). To obtain an optimal capture efficiency
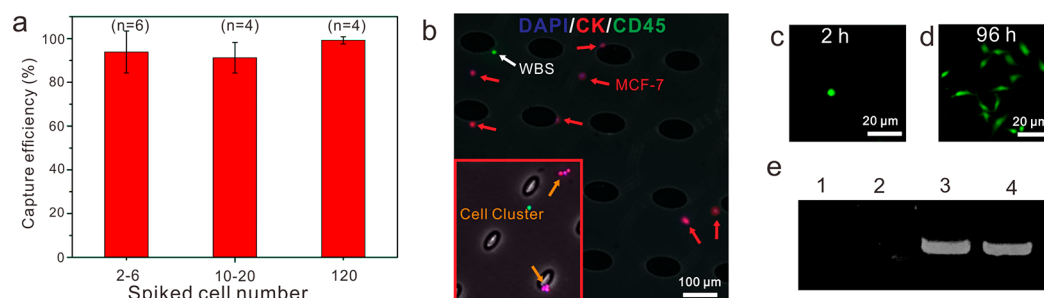
Figure 4. Characterization of the echip. (a) Capture yield of MCF-7 cells spiked into 1 mL of whole blood at concentration from 2 to 120 cells per mL. (b) Fluorescence microscope images of MCF-7 and white blood cells stained with DAPI, cytokeratin, and CD45. (c) Fluorescence microscope image of PC3 cell released from echip for 2 h culturing in a 96-well plate. (d) Representative images of proliferation of a released cell for 4 days. (e) Agarose gel electrophoresis of the products from RT-PCR amplification of PSA mutation. (Lane 1, negative control with sterile water as template; lane 2, negative control of MCF-7 cells; lane3, positive control of PC3 cells; lane 4, PC3 cells captured and lysed in echip.).
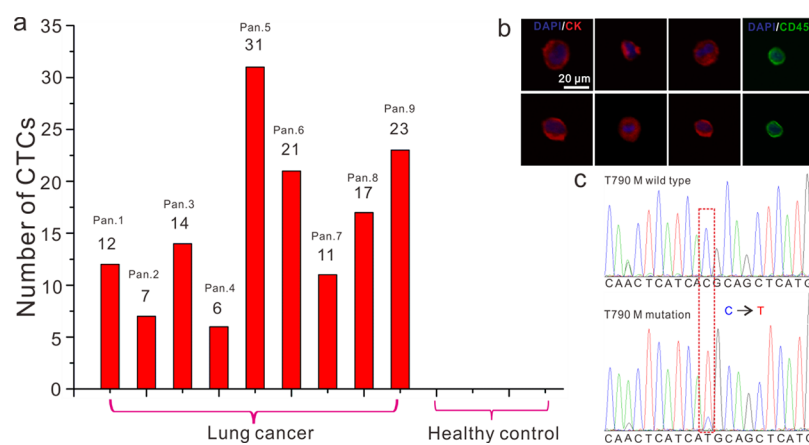
Figure 5. (a) Quantification of CTCs from lung cancer patients. (b) Fluorescence microscope images of CTCs and leukocytes captured from lung cancer patient no. 4 (Pan 4). (c) Identifying T790 M gene mutation (C to T) in the electrochemical released CTCs.

and experimental period, the 160 μm gap and 2 mL/h flow rate were chosen in the following experiments. As showed in Figure 3c, different number of cells (range from 80 to 800) could be recovered with a good linear fitting. Furthermore, the specificity of the echip was evaluated as demonstrated in Figure 3d, the bare and DNA-biotin-modified echip showed a very low capture efficiency compared to the EpCAM modified ones. And as seen in Figure 3e, our EpCAM antibodies modified echip not only could capture high EpCAM expressed cell line (MCF-7 cell), but also the low EpCAM expressed cell line (HepG2 cell) with high efficiency of 96.3% and 85%, respectively. This may because of the hierarchical structures on the channel of our echip that enhanced the interaction with cells. However, the capture efficiency was about 10% for the cervical tumor cell line since no EpCAMs expressed in the HeLa cell. Above results indicated that the echip possessed a low nonspecific capture. The scanning electron microscopy (SEM) images of the MCF-7 cells captured by our echip were illustrated in Figures 3f, S8, and S9. Apart from the MCF-7 and HepG2 cells, the prostatic cancer cells (PC3) and non-small-cell lung cancer (NSCLC) cells (NCI-H1650) were also captured with very high efficiency (more than 90%) by the echip (Figure S10). After investigating the capture efficiency of our echip in buffer system, the ones in human blood samples was explored. Varying number of MCF-7 cells was spiked to 1 mL of whole blood and the resulting solution was flowed through the echip (Figure 4a). Three-color immunocytochemistry (ICC) method was used to distinguish the cancer cell, leukocyte and nucleus, the merged fluorescent

image was showed in Figure 4b. More interesting is that apart from capturing the single cancer cell in whole blood, the cell cluster also could be isolated by our echip (inset of Figure 4b and Figures S8 and S9). The average capture efficiency for 10−20 cells and 120 cells in 1 mL whole blood was 91% and 99%, respectively. Especially worthy of attention, in the case of a few cells (2−6 cells), the average capture efficiency was still more than 93% (Figure 4a). These results confirmed that our echip possessed a very good performance in the cell isolation in the whole human blood. The cell viability after capture and release is very important for the subsequent bioanalysis. As demonstrated in Figure S11, there were only few death cells among the hundreds of the live cells after captured by the echip. Because the echip was electroconductive and the gold−thiol binding chemistry was used to modify the antibody, the captured cells can be easily released by electrochemical method with a high efficiency (Figure S12a and S12b).[32] The released cells possessed a high viability (more than 95%, Figure S12c) and could be cultured and proliferated (Figures 4c, d and S13). The isolated cancer cells could also be directly lysed by the electrochemical method at 20 V for 10 min,[33] and the lysed solution was then collected for the amplification of individual transcripts by PCR with reverse transcription (RT−PCR). As shown in Figure 4e, the prostate-specific antigen (PSA) markers (KLK3) can be detected in the lysed-cell solution from our echip. This RT-PCR result demonstrated that our echip provided a powerful potential for CTC-based molecular analyses.

To further demonstrate the potential of clinical applications of our echip, 4 healthy and 9 lung cancer patient blood samples were flowed through the chip to count the CTCs number. There were different number of CTCs in the 9 patient blood samples wihle there were no detectable cancer cells in the 4 healthy blood samples (Figure 5a, Table S1). The fluorescence images of captured cancer cells and two representative leukocytes from patient no.4 (Pan.4) were shown in Figure 5b. Further genotyping analysis of released CTCs from non-small-cell lung cancer (NSCLC) patients was performed. As demonstrated in Figure 5c, T790 M gene mutation was successfully detected in released CTCs, which is very common in NSCLCs.[34] This preliminary results suggested that our echip had a promising potential for clinical study.

CONCLUSION

In summary, we have successfully demonstrated an electro-conductive micropillar array based chip for highly efficient isolation, release and on-chip electrochemical lysis of rare cancer cells. The hierarchically structured gold layer coating results in a high isolating efficiency and electroconductivity of the chip. The capture efficiency of different cell lines was 85–100% in both buffer and whole blood solution systems. The isolated cells possessed a high viability and can be released intact by electrochemical method with high efficiency for subsequent cell culture or gene mutation detection by sequencing. Furthermore, captured cells could be directly lysed via electrochemical method and the resulted solution can be used for detecting the mutant sites in gene by RT-PCR. Thus, the integrated multifunctional echip with promising applications in clinical diagnosis was well presented.

ASSOCIATED CONTENT

Ⓢ Supporting Information

The Supporting Information is available free of charge on the ACS Publications website at DOI: 10.1021/acs.anal-chem.7b02469.

> XRD pattern, SEM, AFM images, on-chip electrochemical release and cell culture images of chip and information ahout blood samples from patients and healthy human (PDF)

AUTHOR INFORMATION

Corresponding Author

*Tel: 86-27-8779-2203. E-mail: bfliu@mail.hust.edu.cn.

ORCID Ⓞ

Peng Chen: 0000-0002-2392-8106
Yiwei Li: 0000-0002-5203-0290
Bi-Feng Liu: 0000-0002-2135-0873

Author Contributions

§S.Y. and P.C. contributed equally to this work.

Notes

The authors declare no competing financial interest.

ACKNOWLEDGMENTS

REFERENCES

(1) Mehlen, P.; Puisieux, A. *Nat. Rev. Cancer* **2006**, *6*, 449−458.
(2) Pantel, K.; Brakenhoff, R. H.; Brandt, B. *Nat. Rev. Cancer* **2008**, *8*, 329−340.
(3) Alix-Panabieres, C.; Pantel, K. *Clin. Chem.* **2013**, *59*, 110−118.
(4) Yu, M.; Bardia, A.; Aceto, N.; Bersani, F.; Madden, M. W.; Donaldson, M. C.; Desai, R.; Zhu, H.; Comaills, V.; Zheng, Z.; Wittner, B. S.; Stojanov, P.; Brachtel, E.; Sgroi, D.; Kapur, R.; Shioda, T.; Ting, D. T.; Ramaswamy, S.; Getz, G.; Iafrate, A. J.; Benes, C.; Toner, M.; Maheswaran, S.; Haber, D. A. *Science* **2014**, *345*, 216−220.
(5) Krebs, M. G.; Metcalf, R. L.; Carter, L.; Brady, G.; Blackhall, F. H.; Dive, C. *Nat. Rev. Clin. Oncol.* **2014**, *11*, 129−144.
(6) Miyamoto, D. T.; Sequist, L. V.; Lee, R. J. *Nat. Rev. Clin. Oncol.* **2014**, *11*, 401−412.
(7) Zhe, X. N.; Cher, M. L.; Bonfil, R. D. *Am. J. Cancer Res.* **2011**, *1*, 740−751.
(8) Pantel, K.; Alix-Panabieres, C. *Trends Mol. Med.* **2010**, *16*, 398−406.
(9) Zhang, Y.; Wu, M.; Han, X.; Wang, P.; Qin, L. *Angew. Chem., Int. Ed.* **2015**, *54*, 10838−10842.
(10) Nagrath, S.; Sequist, L. V.; Maheswaran, S.; Bell, D. W.; Irimia, D.; Ulkus, L.; Smith, M. R.; Kwak, E. L.; Digumarthy, S.; Muzikansky, A.; Ryan, P.; Balis, U. J.; Tompkins, R. G.; Haber, D. A.; Toner, M. *Nature* **2007**, *450*, 1235−1239.
(11) Wang, L.; Asghar, W.; Demirci, U.; Wan, Y. *Nano Today* **2013**, *8*, 374−387.
(12) Wang, S.; Wang, H.; Jiao, J.; Chen, K. J.; Owens, G. E.; Kamei, K.; Sun, J.; Sherman, D. J.; Behrenbruch, C. P.; Wu, H.; Tseng, H. R. *Angew. Chem., Int. Ed.* **2009**, *48*, 8970−8973.
(13) Yoon, H. J.; Kozminsky, M.; Nagrath, S. *ACS Nano* **2014**, *8*, 1995−2017.
(14) Bhana, S.; Wang, Y. M.; Huang, X. *Nanomedicine* **2015**, *10*, 1973−1990.
(15) Li, Y.; Lu, Q.; Liu, H.; Wang, J.; Zhang, P.; Liang, H.; Jiang, L.; Wang, S. *Adv. Mater.* **2015**, *27*, 6848−6854.
(16) Bole, A. L.; Manesiotis, P. *Adv. Mater.* **2016**, *28*, 5349−5366.
(17) Yan, S.; Zhang, X.; Dai, X.; Feng, X.; Du, W.; Liu, B. F. *ACS Appl. Mater. Interfaces* **2016**, *8*, 33457−33463.
(18) Poudineh, M.; Aldridge, P. M.; Ahmed, S.; Green, B. J.; Kermanshah, L.; Nguyen, V.; Tu, C.; Mohamadi, R. M.; Nam, R. K.; Hansen, A.; Sridhar, S. S.; Finelli, A.; Fleshner, N. E.; Joshua, A. M.; Sargent, E. H.; Kelley, S. O. *Nat. Nanotechnol.* **2016**, *12*, 274−281.
(19) Dharmasiri, U.; Witek, M. A.; Adams, A. A.; Soper, S. A. *Annu. Rev. Anal. Chem.* **2010**, *3*, 409−431.
(20) Wang, S.; Liu, K.; Liu, J.; Yu, Z. T.; Xu, X.; Zhao, L.; Lee, T.; Lee, E. K.; Reiss, J.; Lee, Y. K.; Chung, L. W.; Huang, J.; Rettig, M.; Seligson, D.; Duraiswamy, K. N.; Shen, C. K.; Tseng, H. R. *Angew. Chem., Int. Ed.* **2011**, *50*, 3084−3088.
(21) Yoon, H. J.; Kim, T. H.; Zhang, Z.; Azizi, E.; Pham, T. M.; Paoletti, C.; Lin, J.; Ramnath, N.; Wicha, M. S.; Hayes, D. F.; Simeone, D. M.; Nagrath, S. *Nat. Nanotechnol.* **2013**, *8*, 735−741.
(22) Ke, Z.; Lin, M.; Chen, J. F.; Choi, J. S.; Zhang, Y.; Fong, A.; Liang, A. J.; Chen, S. F.; Li, Q.; Fang, W.; et al. *ACS Nano* **2015**, *9*, 62−70.
(23) Lin, M.; Chen, J. F.; Lu, Y. T.; Zhang, Y.; Song, J.; Hou, S.; Ke, Z.; Tseng, H. R. *Acc. Chem. Res.* **2014**, *47*, 2941−2950.
(24) Poudineh, M.; Labib, M.; Ahmed, S.; Nguyen, L. N. M.; Kermanshah, L.; Mohamadi, R. M.; Sargent, E. H.; Kelley, S. O. *Angew. Chem., Int. Ed.* **2017**, *56*, 163−168.
(25) Lv, S. W.; Liu, Y.; Xie, M.; Wang, J.; Yan, X. W.; Li, Z.; Dong, W. G.; Huang, W.-H. *ACS Nano* **2016**, *10*, 6201−6210.
(26) Li, W.; Reátegui, E.; Park, M. H.; Castleberry, S.; Deng, J. Z.; Hsu, B.; Mayner, S.; Jensen, A. E.; Sequist, L. V.; Maheswaran, S.; et al. *Biomaterials* **2015**, *65*, 93−102.
(27) Yu, X.; Wang, B.; Zhang, N.; Yin, C.; Chen, H.; Zhang, L.; Cai, B.; He, Z.; Rao, L.; Liu, W.; Wang, F. B.; Guo, S. S.; Zhao, X. Z. *ACS Appl. Mater. Interfaces* **2015**, *7*, 24001−24007.
(28) Wang, J.; Li, W.; Zhang, L. C.; Ban, L.; Chen, P.; Du, W.; Feng, X. J.; Liu, B. F. *ACS Appl. Mater. Interfaces* **2017**, *9*, 27441−27452.

(29) Wang, J.; Li, W.; Lu, Z. C.; Zhang, L. C.; Hu, Y.; Li, Q. B.; Du, W.; Feng, X. J.; Liu, B. F.; et al. *Nanoscale* **2017**, *9*, 15598.

(30) Green, B. J.; Saberi Safaei, T.; Mepham, A.; Labib, M.; Mohamadi, R. M.; Kelley, S. O. *Angew. Chem., Int. Ed.* **2016**, *55*, 1252−1265.

(31) Chen, Y.; Li, P.; Huang, P. H.; Xie, Y.; Mai, J. D.; Wang, L.; Nguyen, N. T.; Huang, T. J. *Lab Chip* **2014**, *14*, 626−645.

(32) Zhang, P.; Chen, L.; Xu, T.; Liu, H.; Liu, X.; Meng, J.; Yang, G.; Jiang, L.; Wang, S. *Adv. Mater.* **2013**, *25*, 3566−3570.

(33) Mohamadi, R. M.; Ivanov, I.; Stojcic, J.; Nam, R. K.; Sargent, E. H.; Kelley, S. O. *Anal. Chem.* **2015**, *87*, 6258−6264.

(34) Yun, C. H.; Mengwasser, K. E.; Toms, A. V.; Woo, M. S.; Greulich, H.; Wong, K. K.; Meyerson, M.; Eck, M. J. *Proc. Natl. Acad. Sci. U. S. A.* **2008**, *105*, 2070−2075.